

Stability-transport modeling of the SINP tokamak discharges

S LAHIRI, S MUKHOPADHYAY, A N S IYENGAR and R PAL

Plasma Physics Group, Saha Institute of Nuclear Physics, 1/AF Bidhan Nagar, Calcutta 700 064, India

MS received 26 June 2000; revised 9 January 2001

Abstract. A one-dimensional stability transport code has been developed to simulate the evolution of tokamak plasma discharges. Explicit finite-difference methods have been used to follow the temporal evolution of the electron temperature equation. The poloidal field diffusion equation has been solved at every time step. The effects of MHD instabilities have been incorporated by solving equations for MHD mixing and tearing modes as and when required. The code has been applied to follow the evolution of tokamak plasma discharges obtained in the Saha Institute of Nuclear Physics (SINP) tokamak. From these simulations, we have been able to identify the possible models of thermal conductivity, diffusion and impurity contents in these discharges. Effects of different MHD modes have been estimated. It has been found that in low q_a discharge $m = 1$, $n = 1$ and $m = 2$, $n = 1$ modes play major role in discharge evolution. These modes are found to result in the positive jump in the loop voltage which was also observed in the experiments. Hollow current density profile j_ϕ and negative shear in the q profile have also been found in the rising phase of a discharge.

Keywords. Transport; stability; diffusion; MHD.

PACS No. 52.65.-y

1. Introduction

Computer simulation has been found to be extremely successful in exploring intricate physical phenomena, and thus help in a better understanding of experimental situations. A full description of the plasma behaviour would require a three dimensional calculation [1]. But such studies are extremely complicated and need a lot of computational power and time. Moreover, it is sometimes very important to know the detailed parametric variation of a particular discharge. For this purpose, a one-dimensional (1D) code has been found to be quite sufficient [2,3]. Considering the above, we have attempted to develop a simple one-dimensional numerical model to simulate the evolution of j_ϕ profile and related parameters for different discharges obtained in the SINP tokamak. Low q_a discharges ($q_a < 2$ and $q_a < 1$) have been setup in the SINP tokamak [4,5], and it is seen that the current rise phase plays an important role in the accessibility and evolution of these discharges [5–7]. In this paper, the principal aim of study was to simulate the current density profile evolution in the rising phase of the low q_a discharges obtained experimentally in the SINP tokamak.

2. Description of the present model

The geometry of the model [3] is cylindrical and is applicable to a tokamak provided the aspect ratio is sufficiently large. In the SINP tokamak, the aspect ratio can be varied from 4(30 cm/7.5 cm) to ≈ 5.5 (30 cm/5.5 cm). So the model is well applicable to it. The model is divided into two parts: (1) transport and (2) stability. Method of solution is as follows:

(i) We integrate the system of equation of energy and magnetic field diffusion, checking at each time step for the appearance of resonant surfaces and the fulfillment of the stability conditions.

(ii) If at any moment, a resonant surface appears and it is found that a stability calculation is necessary, we interrupt the integration of the system and perform the stability calculation and appropriate estimation of all the required quantities such as thermal conductivity, diffusivity, resistivity of plasma etc.

(iii) After calculating the above mentioned quantities, we continue the integration of the system of equations representing transport.

2.1 Transport model

In this model, we have considered two coupled differential equations (1) and (2) where eq. (1) is the poloidal magnetic field (B_θ) diffusion equation and eq. (2) is the electron temperature (T_e) evolution equation. The diffusion equation is written as

$$\frac{\partial B_\theta}{\partial t} = \frac{\partial E(r)}{\partial r}, \quad (1)$$

where $E(r)$ is the axial electric field. The temperature evolution is represented by

$$\frac{\partial T_e}{\partial t} = \frac{1}{3n_e} \times \left[jE + \frac{1}{r} \times \frac{\partial}{\partial r} \left(rn_e \chi_e \frac{\partial T_e}{\partial r} + \frac{5}{2} r T_e D_e \frac{\partial n_e}{\partial r} \right) - R(T) \right], \quad (2)$$

where j , χ , D and R are the current density, thermal conductivity, diffusion and the radiation loss factors respectively. The boundary conditions for eq. (2) are $\partial T_e / \partial r = 0$, at $r = 0$ and $T_e = T_a$ at $r = a_p$, where T_a is the edge value of temperature, a_p is the minor radius of the plasma. In addition to the above two equations, the MHD mixing [9] and the tearing mode equation [13] has been solved as and when required to incorporate the effects of the instabilities. It has been assumed that the density profile does not vary in time and is expressed by $n(r) = n_0 + n_1(1 - r^2/a_p^2)$, where n_0 is the density at the edge of the plasma and $n_0 + n_1$ is the density at the centre of the plasma. The parameters χ_e and D_e are obtained as $\chi_e = \chi_{e0} + \chi_{eI}$ and $D_e = D_{e0} + D_{eI}$, where the term with subscript 'e0' is the value without considering the effect of instability and the other term with subscript 'eI' is the effect due to instability. Explicit finite-difference scheme has been used to solve these equations. As a result, it has become necessary to conform to strict stability criterion. In particular, time stepping has been carried out using the largest possible time step Δt which satisfies $\frac{2\eta\Delta t}{\mu_0 a_p (\Delta r)^2} < 1$ where Δr is the grid size in the radial direction, η is plasma resistivity and μ_0 is the permeability of the vacuum.

2.2 Stability analysis

In order to incorporate the effect of MHD instabilities, resistive analysis has been carried out to follow the growth and decay rates of a large number of MHD modes. The effects of these instabilities have been incorporated in the calculations through their effect on thermal conductivity, diffusion coefficient and resistivity using the following approaches:

(1) *Empirical*: According to this method, the effects of the instabilities were incorporated in the form of empirical equations when the current profile was hollow and the local minimum in q is near integral, i.e., $0 < (m/n - q_{\min}) < 0.1$ [8]. At each resonant surface,

$$\chi_{eI} = \text{constant} \times \chi_{e0},$$

D_{eI} has been considered in the same manner.

(2) *MHD mixing*: Rapid mixing of the poloidal field, density and temperature of particles in a particular layer can occur in the plasma due to the existence of a resonant surface inside the plasma which destroys the magnetic surface configuration partially. Generally, the mixing time is much smaller than the characteristic times for thermal conduction and diffusion. Kadomtsev's model has been used for this part of the analysis [9] which follows the evolution and mixing of the flux function ψ which represents the deviation of the poloidal magnetic flux from the flux created by a uniform field. Mathematically, this function can be described as

$$\psi = -\frac{1}{R} \int_0^r (1/q - n/m) r dr.$$

The experimentally observed mixing has been roughly divided into (i) internal mixing (occurring in the central region), and (ii) external mixing (occurring on the plasma periphery). Instabilities due to the existence of both single (SRS) and double (DRS) resonant surfaces have been considered in this model. The expression of χ_{eI} according to this model is

$$\chi_{eI} = \chi_c \left(1 - \left(\frac{x_{\text{mix}}}{h_{\text{mix}}} \right)^2 \right)$$

with $\chi_c \gg \chi_{e0}$. Here, x_{mix} is the distance from the centre of the mixing region and h_{mix} is the half width of the mixing region.

(3) *Resistive stability analysis*: Instabilities have been taken into consideration using the equation

$$\frac{1}{r} \frac{d}{dr} \left(r \frac{d\psi}{dr} \right) - \frac{m^2}{r^2} \psi - \frac{dj_\phi/dr}{\mu_0 \left(1 - \frac{nq}{m} \right)} \psi = 0, \quad (3)$$

where poloidal flux function $\psi = \frac{irB_r}{m}$, B_r is the perturbed radial magnetic field, q is the safety factor. Both the SRS [2] and DRS [10] modes have been handled using proper boundary conditions. The solution has been considered to have converged only when the difference between the ψ in the previous iteration and that in a particular iteration is less than 1.0×10^{-6} . While simulating the experimental situations, a large number of modes, namely, 4/1, 3/1, 2/1, 3/2, 1/1, 4/5, 3/4 have been considered. Depending on the SRS

and DRS behaviour of a particular mode, proper boundary conditions have been set up and growth rates of the modes have been estimated. Growth of the mode and related islands have been estimated following Rutherford's theory [11] according to which the mode ceases the exponential growth and enters a domain of algebraic growth as soon as the island is larger than the tearing layer. Across the island region of each tearing mode, χ_{eI} has been estimated to be given as

$$\chi_{eI} = \chi_c \left(1 - \left(\frac{x_s}{h} \right)^2 \right),$$

where x_s is the distance from the island centre and h is the island half width. For the above calculations a perfectly conducting wall has been assumed to be situated at 8.5 cm from the plasma centre which is the radius of the vacuum vessel of the SINP tokamak.

Analysing the results from a large number of computations, it was also possible to arrive at an optimum method for estimating the effects of instabilities. It is as follows:

- (i) $m = 1, n = 1$ modes to be handled empirically.
- (ii) All other SRS modes to be handled by the tearing mode solver.
- (iii) All DRS modes to be handled by mixing theory (in principle, it can also be done by the tearing mode solver but the convergence process becomes extremely slow in such a case).
- (iv) Under certain circumstances, it is possible to have more than two resonant surfaces at the same instant. This is a rather complicated situation and can be either taken care of by using the empirical approach or may have to be neglected altogether.

The transport and the stability model has been validated using well-known theoretical equations [12,13].

3. Results

3.1 Parametric studies

Different models (diffusion, thermal conductivity, radiation etc) suitable for explaining the SINP tokamak discharges have been obtained through an extensive numerical scan of the available parameters of eq. (2). During these scans, all the parameters, except one was kept constant. This particular parameter (χ , D or R) was varied according to different models, or different quantities (impurity content). In each case, temperature profile and other parameters obtained from simulation were studied critically to see if there was some unrealistic result. Since we were not simulating an exact experimental scenario, the total plasma current was also kept constant during the scans (≈ 10 kA) and only the transport model has been considered for this purpose. The effects of the instability have not been taken into consideration.

For thermal conductivity, we have considered models from [13–18]. It has been seen that Ohkawa model [18] for thermal conductivity is suitable for the SINP tokamak. Thus,

$$\chi_e \approx \frac{c^2}{\omega_{pe}^2} \frac{v_e}{qR_0}, \quad (4)$$

where $\omega_{pe} = \sqrt{\frac{4\pi e^2 n_e}{m_e}}$ is the plasma frequency and $v_e = \sqrt{\frac{2T_e}{m_e}}$ is the mean electron thermal velocity. Thus eq. (4) has been written in C.G.S. system of units.

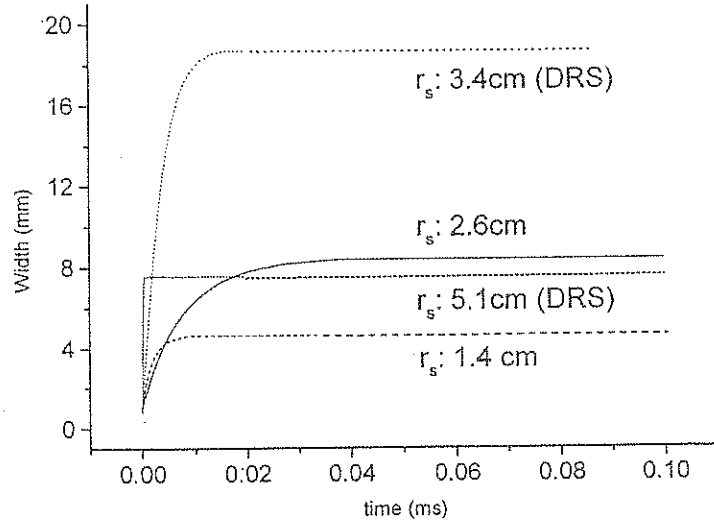


Figure 1. Hollow j_ϕ profile, $B_t = 0.308$ T, $a_t = 5.5$ cm, $r_s = 1.4$ cm for $I_p = 10.0$ kA (SRS), $r_s = 2.6$ cm for $I_p = 8.0$ kA (SRS), $r_s = 3.4$ cm and $r_s = 5.1$ cm for $I_p = 7.0$ kA (DRS).

For diffusion coefficient, we considered different models [19], e.g., the classical model, the Pfirsch–Schluter model, the neo-classical model, the Kadomtsev model and the Bohm model. Similarly, Bohm model has been found suitable for diffusion part. The Bohm diffusion coefficient (D_B) is estimated by the equation

$$D_B = \frac{1}{16} \frac{T_e}{e B n_e}. \quad (5)$$

Going through numerical experiments, we concluded that a satisfactory model of impurity distribution for the SINP tokamak low q_a plasma may be the following: (1) The distribution approximately follows the plasma density distribution. (2) Low Z impurities remain below 2%. (3) High Z impurities remain below 0.5%.

3.2 Island width calculations

For various constant current cases, we tried to estimate the growth of islands related to various modes. One of the representative results for the $m = 2$ mode has been illustrated in figure 1 which is for a hollow current density profile, with $B_t = 0.308$ T and $a_t = 5.5$ cm. The first one is for $I_p = 10$ kA, second one is for $I_p = 8$ kA and the third one is for $I_p = 7$ kA. The q_a in these cases are 1.55, 1.94 and 2.2. The positions of the resonant surfaces are at 1.4 cm, 2.6 cm from the centre of the vessel in the first two cases. At 7 kA we are getting double resonant surfaces for $m = 2$, $n = 1$ mode at 3.4 cm and 5.1 cm. Initially the islands are found to grow very fast and after that it saturates. The width of the island in the case where the resonant surface is at 3.4 cm (DRS) is around 2 cm. This value is remarkably close to that obtained from the external magnetic probes in the SINP tokamak [20].

3.3 Effect of the rate of plasma current rise on the profile evolution

The effect of the rate of current rise on the shape of the current density profile and other plasma parameters have been studied using the developed code. In this study, we have not considered the effects of the instability on various plasma parameters. Figure 2a and 2b show the evolution of the current density profile for a slow ($\dot{I}_p = 5$ mA/s) and a fast $\dot{I}_p = 50$ mA/s rate of current rise, respectively. According to figure 2a, the initial flat j_ϕ profile retains a more or less flat shape in $15 \mu\text{s}$, while in figure 2b, j_ϕ profile changes its initial flat shape and changes to a subsequently hollow profile within the same time span. The study confirms the knowledge that, larger \dot{I}_p results in a stronger skin effect where a large percentage of the total current remains close to the plasma edge. This is a verification of our experimental findings reported elsewhere [7].

3.4 Application to experimental situations

3.4.1 Experimental scenario: Using the experience gained in the previous simulations, the experimental scenario of a large number of SINP tokamak discharges were reconstructed. In order to carry out these simulation, the value of the total plasma current at each instant

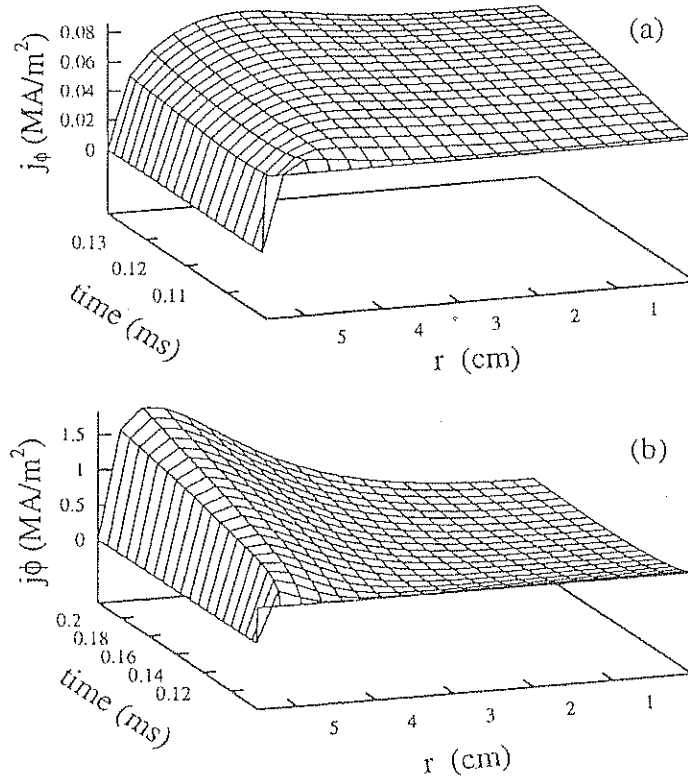


Figure 2. The effect of the rate of rise of I_p . (a) Slow current rise, (b) fast current rise.

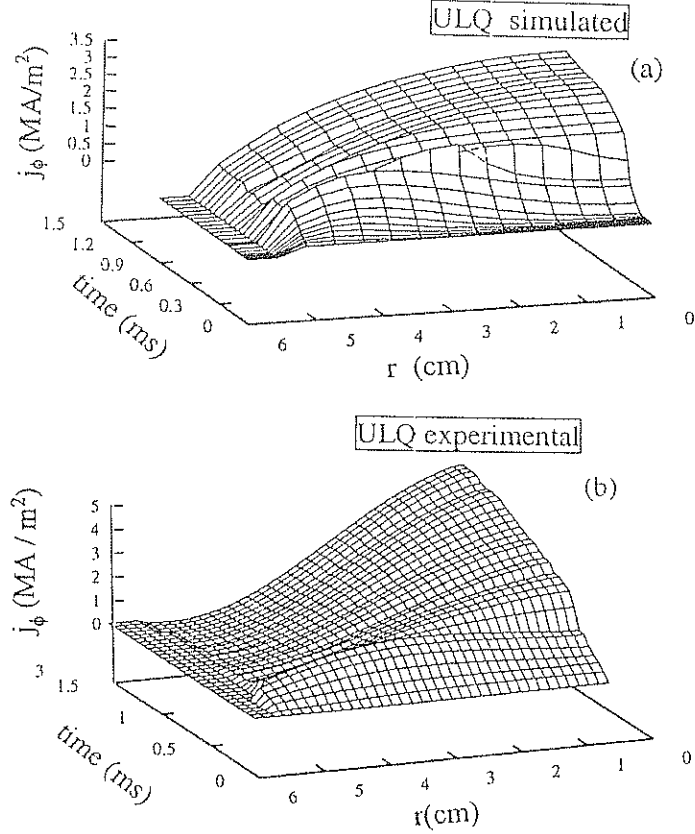


Figure 3. j_ϕ profile of the ULQ discharge obtained from (a) simulation, (b) experiment.

(obtained experimentally) was supplied as an input. Here, we have presented representative results for one discharge with $q_a = 0.8$. The various parameters were as follows: major radius: 0.3 m, minor radius: 0.055 m, toroidal magnetic field: 0.308 T (ULQ) and 0.88 T for (NQ), plasma particle density at the centre: $2 \times 10^{19} \text{ m}^{-3}$, plasma particle density at the edge: $1 \times 10^{18} \text{ m}^{-3}$, thermal conductivity: Ohkawa model, diffusion: Bohm model, impurity content: carbon: 2.0 %, oxygen: 2.0 %, iron: 0.5 %, tungsten: 0.5 %, modes considered: 4/1, 3/1, 2/1, 3/2, 1/1, 4/5, 3/4, 2/3, 1/2. Simulated results of the ultra low q_a discharge are shown in figures 3 to 6. The experimental results have also been produced along with these simulated ones. Figure 3a shows the j_ϕ profile obtained from simulation while figure 3b shows the experimentally obtained j_ϕ profile. Both the figures have been drawn for a time slice of 1.5 ms from the initiation of the discharge. In the experiment (figure 3b), the initial hollow shape is sustained for around $350 \mu\text{s}$, then it changes to a parabolic one. In the simulation, the initial j_ϕ profile was considered to be flat and it has been allowed to evolve with time. In simulation also, the j_ϕ profile changes its shape around $300 \mu\text{s}$ and moves towards a more parabolic one as time passes. The order of magnitude of j_ϕ are almost the same in both the cases ($\approx 4.0 \times 10^6 \text{ amp/m}^2$). In the loop voltage obtained experimentally a positive jump is usually obtained around $300 \mu\text{s}$. This

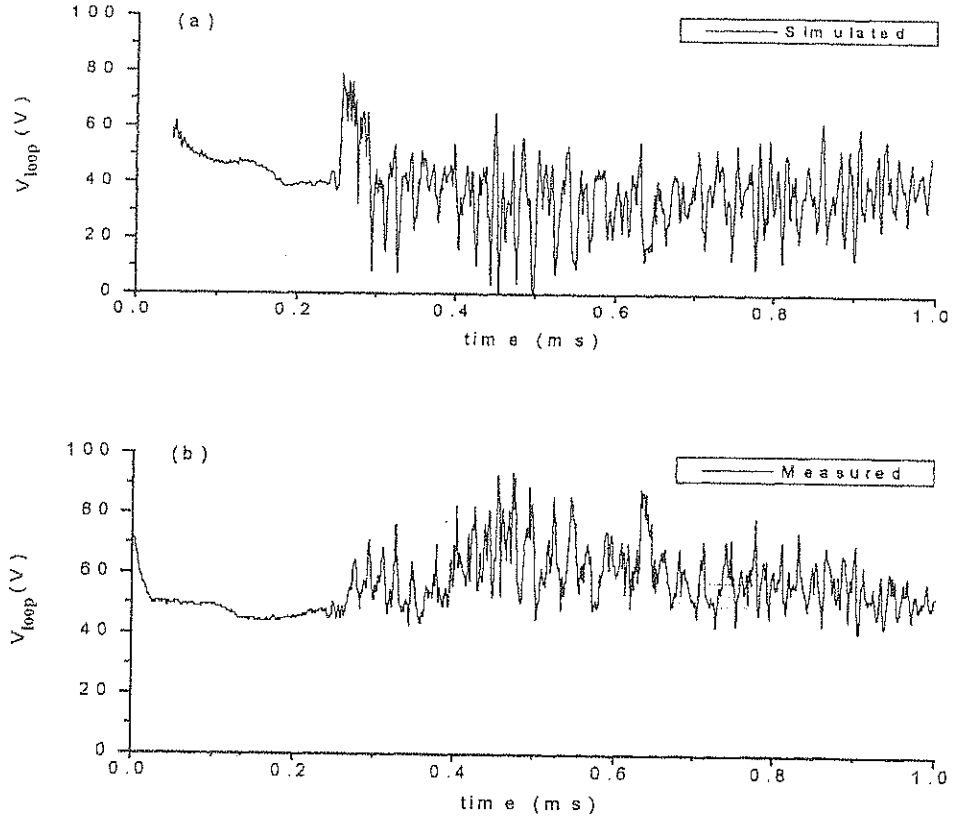


Figure 4. Loop voltage of the ULQ discharge obtained from (a) simulation, (b) experiment.

positive jump is found to be connected with the shape change in the j_ϕ profile. Figures 4a and 4b show the loop voltage obtained from simulation and experiment respectively. It is seen that the spikes in the loop voltage obtained experimentally has been reproduced by our very simple model. The positive spikes in the loop voltage starts around $250 \mu\text{s}$ and this continues up to $350\text{--}400 \mu\text{s}$ and has a magnitude of 70 volt according to figure 4b. The same positive spike appears in the simulated loop voltage around $250 \mu\text{s}$ and continues up to $300 \mu\text{s}$. After that again bunch of spikes start. It has been seen from the experiment and the simulations that $m = 1, n = 1$ mode is associated with this positive jump and this changes the shape of the current density profile. The simulated T_e and q profiles are shown in figures 5 and 6 respectively. The central temperature is around 100 eV. Initially the T_e profile is hollow and as time passes it changes to a parabolic shape. The q profile also shows negative shear up to $350 \mu\text{s}$ and after that it increases monotonically. The change in shape of j_ϕ and q indicates current penetration towards the plasma current column.

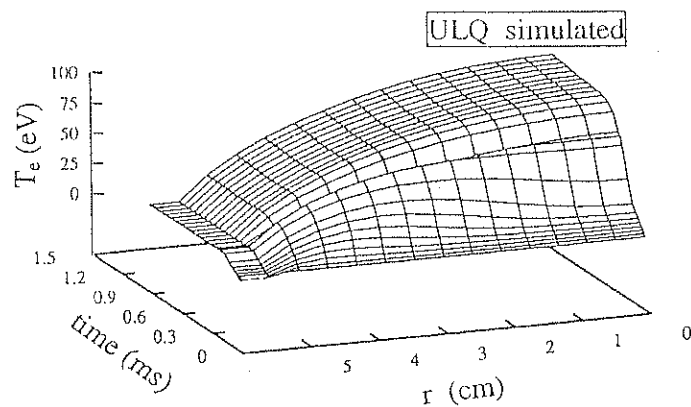


Figure 5. Simulated T_e profile.

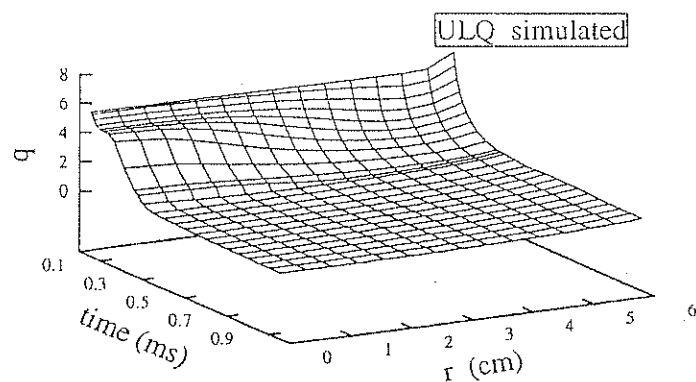


Figure 6. Simulated q profile.

4. Conclusions

The current penetration problem is a highly nonlinear one, involving a competition between current diffusion, ohmic heating, thermal transport and stability. Despite the simplicity of the numerical model, it is found that the simulation reproduced the global features of the experimental observations.

- (i) The thermal conductivity of the SINP tokamak plasmas seems to follow the empirical relations similar to those described by the Ohkawa model [18].
- (ii) It is well-known that the plasma diffusion follows the Bohm model in the early phase of a discharge [17]. The diffusion in the other phases of the low q_a discharges in the SINP tokamak also seems to be described well by the Bohm model because these are fluctuation dominated.
- (iii) There is a good amount of low Z impurities in the plasma, although the amount of high Z impurities should be quite low.

- (iv) High rate of current rise allows the j_ϕ profile to remain hollow for a longer time; during this period, various instabilities may attempt to destabilize the plasma but none of them can grow to a sufficiently large magnitude.
- (v) We plan to improve the code by incorporating the following phenomena:
 - (a) anomaly in the values of χ , η and D may be present during the discharge evolution (especially in the fluctuation dominated ULQ regime),
 - (b) surface wall interaction,
 - (c) ion temperature evolution and density evolution,
 - (d) interaction among different modes.

Acknowledgement

This article was presented at the Proceedings of the Fourteenth National Symposium on Plasma Science and Technology, Amritsar.

References

- [1] K Kusano, T Sato, H Yamada, Y Murakami, Z Yoshida and N Inoue, *Nucl. Fusion* **28**, 89 (1988)
- [2] L Giannone, R C Cross and I H Hutchinson, *Nucl. Fusion* **27**, 2085 (1987)
- [3] M F Turner and J A Wesson, *Nucl. Fusion* **22**, 1069 (1982)
- [4] A N Sekar Iyengar, S K Majumdar, J Basu, R K Paul and S Chowdhury, *Pramana – J. Phys.* **39**, 181 (1992)
- [5] S Lahiri, A N Sekar Iyengar, S Mukhopadhyay and R Pal, *Nucl. Fusion* **36**, 254 (1996)
- [6] S Lahiri, S Mukhopadhyay, A N Sekar Iyengar and R Pal, *IEEE Trans. Plasma Sci.* **25**, 509 (1997)
- [7] S Lahiri, A N Sekar Iyengar, S Mukhopadhyay and R Pal, *Pramana – J. Phys.* (communicated)
- [8] R S Granetz, I H Hutchinson and D C Overskei, *Nucl. Fusion* **19**, 1587 (1979)
- [9] Y N Dnestrovskii and D P Kostomarov, *Numerical simulation of plasmas* (Springer-Verlag, Berlin, Heidelberg, 1986)
- [10] G Urquijo, N Persson and E K Maschke, *Nucl. Fusion* **34**, 1299 (1994)
- [11] P H Rutherford, *Phys. Fluids* **16**, 1903 (1973)
- [12] R J Goldston and P H Rutherford, *Introduction to plasma physics* (Institute of Physics Publishing, Bristol and Philadelphia, 1995) p. 139
- [13] J Wesson, *Tokamaks* (Clarendon Press, Oxford, 1987)
- [14] L A Artsimovich, *Pis'ma Zh. Eksp. Teor. Fiz.* **13**, 101 (1971)
- [15] D L Jassby, D R Cohn and R R Parker, *Nucl. Fusion* **16**, 1045 (1976)
- [16] B B Kadomtsev, *Fiz. Plazmy* **9**, 938 (1983)
- [17] V M Leonov, V G Merezkin, V S Muchorotov, V V Sannikov and G N Tiliin, Plasma physics and controlled nuclear fusion research, *Proc. Brussels* (IAEA, Vienna, 1981) vol. 1, p. 393
- [18] T A Ohkawa, *Phys. Lett.* **A67**, 35 (1978)
- [19] K Miyamoto, *Plasma physics for nuclear fusion* (The MIT Press, 1980)
- [20] A N S Iyengar, R Pal, S Lahiri and S Mukhopadhyay, *Nucl. Fusion* **38**, 1177 (1998)